Elastic light scattering from semiconductor structures: Localized versus propagating intermediate electronic excitations

V. I. Belitsky, A. Cantarero, and S. T. Pavlov*
Departamento de Física Aplicada, Universitat de València, Burjassot, E-46100 València, Spain

M. Gurioli, F. Bogani, A. Vinattieri, and M. Colocci
Dipartimento di Fisica dell'Università di Firenze and LENS, 50125 Firenze, Italy
(Received 20 June 1995)

We present a theoretical study of the relative role of localized and propagating intermediate electronic states in the processes of elastic scattering of light. Only localized excitations lead to isotropic scattering in lowest-order perturbation theory. Inhomogeneous broadening of the optical transition affects the scattering efficiency from the ordered and disordered array of localized states in a qualitatively different way. The propagating electronic excitations may only contribute to elastic light scattering via higher-order processes. The scattering of excitons by impurities or the interface roughness potential is suggested as a mechanism for the contribution of propagating excitations. An analysis of experimental data on elastic scattering of light from quantum-well structures and bulk semiconductors suggests that the bulk materials, rather than widely investigated quantum wells, are favorable systems for studying the role of propagating electronic excitations.

I. INTRODUCTION

After the work of Hegarty *et al.*,[1] the processes of elastic scattering of light have attracted considerable attention, especially in the investigations of semiconductor-based low-dimensional structures.[1–6] This is mainly because of the possibility of distinguishing between homogeneous and inhomogeneous broadening of the electronic excitations participating in the scattering process. Progress in time-resolved spectroscopy has recently stimulated theoretical analysis of the time dependence of the scattering efficiencies.[3–7]

In semiconductor-based quantum-well (QW) structures, inhomogeneous broadening is mainly due to the interface roughness which may result in a considerable spatial fluctuation in the energy of the size-quantized electronic states. In light scattering experiments, these fluctuations are not important when the frequency of incident light is far from resonance with the electronic excitations.[1,8–12] The relatively small difference in energy of excitations leads then to a small correction to the scattering efficiency of a perfect superlattice (SL). However, under resonant conditions, the states having the energy most close to the laser frequency are selectively excited with dramatic effects even for small fluctuations[1,8–12] and the scattering efficiency acquires features typical of the disordered systems; the relative strength of the SL and single QW features provides information on the homogeneous and inhomogeneous broadening.[1,8–12]

The enhancement of the effects of disorder under resonant excitation is common to both elastic and inelastic scattering processes. However, while detailed models have been developed for the analysis of the inelastic light scattering, a microscopic theory of the resonant Rayleigh scattering (RRS) is still missing. In particular, no special attention has been paid so far to the question of the relevant intermediate electronic states, even if the localized *or* propagating character of electronic excitations available for the scattering process results in an important difference in the scattering mechanism. In this paper, we develop a theoretical approach to the RRS, based on the evaluation of the scattering efficiency via a quantum-mechanical calculation of the scattering amplitude. This allows us to demonstrate that only localized electronic excitations (LEE's) contribute to the RRS in the lowest-order perturbation theory (see, also, Ref. 6), whereas a nonzero contribution from propagating electronic excitations (PEE's) appears in higher-order processes.

A key role in the RRS process is obviously played by disorder. The disorder enters in two different ways in the light scattering process: It is responsible for the inhomogeneous broadening and spatial disorder of LEE's, on one hand, and leads to finite contributions to the RRS efficiency of PEE's via higher-order processes, on the other. A number of parameters are, therefore, important for observing a RRS signal: the inhomogeneous broadening and/or the spatial disorder as far as the scattering by *localized* electronic excitations is concerned, and the concentration of defects and/or the strength of the random potential related to the interface roughness, effective in the elastic scattering of the PEE's, in the case of RRS via *propagating* states. Furthermore, the coherent character of the contributions to the scattering amplitude from individual localized states, along with spatial and energy fluctuations, leads to a number of qualitatively different regimes for the RRS, as analyzed in details in the following.

It is important to note that the meaning of inhomogeneous broadening, in this paper (and in Refs. 1 and

8–12), is different from that considered, for example, in a recent publication of Glutsch and Bechstedt.[13] In our approach, the average of the scattering efficiency for a QW structure is to be taken over different realizations of the size-quantized energies of individual QW's. The inhomogeneous broadening comes from a spatial distribution of partially or totally localized electronic excitations with different *size-quantized energies*. Our approach for the states delocalized solely in one or two directions is valid only for large-scale disorder, such as growth islands in QW structures that was not the subject of Ref. 13. The inhomogeneous broadening in the sense of Ref. 13 follows from the interaction of *propagating* electronic excitations with a random potential in a QW and leads, after the averaging, to broadening in a Green function of the electronic state. This mechanism can be included in our calculation through the dressing of electronic propagators. In fact, as long as the Green function of a PEE of the individual QW preserves its diagonality in wave vector (see, e.g., Ref. 13), there is no contribution to the Rayleigh scattering in the *lowest-order* (see the next section) perturbation theory. Being arranged as a multiple QW structure, such a system is a perfect SL, since all individual QW's are indistinguishable.

We also present experimental data on single QW and bulk semiconductor structures. We find that in a QW, the RRS mainly occurs via excitons localized at the interface roughness, as indicated by the redshift of the RRS profile with respect to the fundamental excitonic transition. In the case of a bulk GaAs, the situation seems to be more interesting, even if less clear. The RRS signal turns out to be unshifted, with respect to the exciton transition, and the resonant contribution from excitons bound to a donor is resolved as well. On one side, our findings confirm that RRS is selectively sensitive to localized states; on the other side, it may suggest that bulk materials, rather than the more widely investigated QW's, can provide the appropriate systems for studying the RRS via propagating excitonic states. In fact, the interface roughness, which is the main mechanism producing localization in QW's, is missing in bulk samples.

The paper is organized as follows. A general consideration of the selection rules for wave vector and its consequences for RRS are given in Sec. II. The scattering by localized and propagating electronic states are considered in Secs. III and IV, respectively. Section V reports a few experimental observations and the concluding remarks are given in Sec. VI.

II. GENERAL CONSIDERATION

The RRS efficiency can be evaluated in the lowest-order perturbation theory with the help of the diagram shown in Fig. 1(a). The terms "lowest-" or "higher-order perturbation theory" refer to the expansion over any kind of *elastic* interaction coupling the left and right hand sides of the diagram for scattering *efficiency* (not for scattering amplitude). Hence, the diagram in Fig. 1(a) is of zero order, while those in Fig. 1(b) represent higher-order contributions. At the same time, all electronic intermediate states are assumed to be renormalized by all relevant interactions. The dashed lines on the left and right hand side of a diagram correspond to an incident photon and are labeled by its frequency ω_l and wave vector $\vec{\kappa}_l$. The dashed line in the middle of the diagram represents the scattered light ($\vec{\kappa}_s$, ω_s). There are no other excitations in the final state, because of the elastic character of the scattering process. The double lines in both parts of the diagram represent an intermediate electronic excitation, which is created in the absorption event and recombines with the emission of a scattered photon. Intermediate excitation can be either real or virtual, depending on the energy of the incident light quantum. However, it is assumed that the laser frequency is close to resonance with the electronic excitation, so that the diagram with crossing photon lines of the incident and scattered light may be neglected.

The scattering efficiency for the process of Fig. 1(a) can be written as[14]

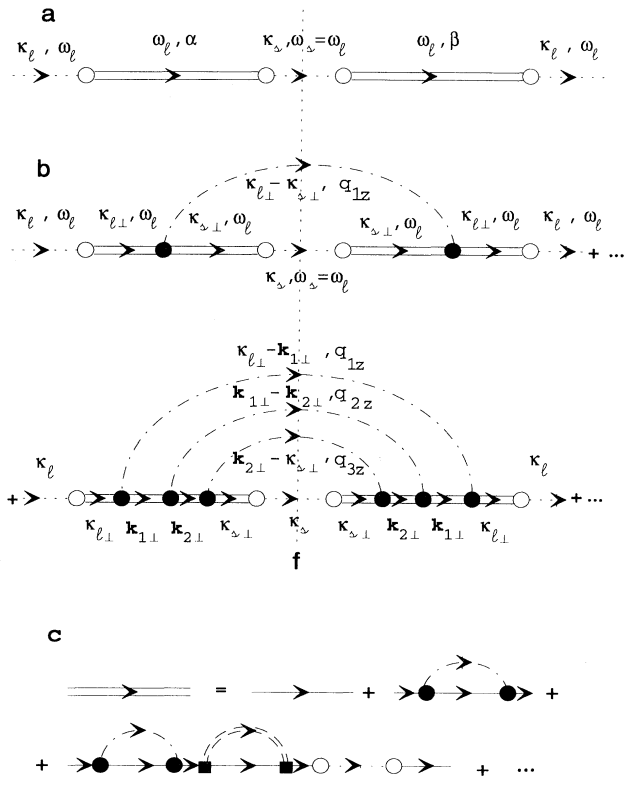

FIG. 1. Zero (a) and higher (b) order diagrams for the Rayleigh scattering efficiency. Double lines correspond to the relevant type of intermediate electronic excitations and are labeled by the total set of corresponding quantum numbers. Dash-dotted lines represent interaction with defects. All variables in (b) are taken for scattering from multiple quantum-well structure. (c) Diagrams contributing to the dephasing of a propagating exciton. The double dash line represents the interaction with a phonon and the dashed line takes account of radiative broadening.

$$I_s(\omega_l) \sim \sum_{\alpha\beta} G(\omega_l;\alpha)G^*(\omega_l;\beta)\delta(\omega_s - \omega_l), \qquad (1)$$

where the indices α and β represent the whole set of quantum numbers for intermediate electronic states and $G(\omega;\alpha)$ is the Green function of the electronic excitation. In principle, $G(\omega;\alpha)$ is the solution of a Dyson equation that takes into account all the relevant interaction mechanisms. This leads to broadening and renormalization of the intermediate states. An example of diagrams contributing to the dressing of electronic excitations is shown in Fig. 1(c), where the dash-dotted line corresponds to the scattering by disorder, the double dash line describes an inelastic scattering by phonons, and the inclusion of the dashed line for photon accounts for radiative recombination. Such processes are responsible for a dephasing.

The scattering efficiency for processes of Fig. 1(b) can be written in a similar way. The selection rules for quasimomentum follow from the matrix elements of interaction of the electronic subsystem with light (open circles) and disorder (full circles), respectively, and depend strongly on the type of relevant electronic states. It is important to note that the dash-dotted lines for scattering by disorder appear in the diagrams of Fig. 1 in two different ways: there are *internal* lines contributing to dephasing of electronic excitations and *external* lines responsible for RRS by PEE's. All external lines are crossed by the vertical line f corresponding to the final state of the system. We emphasize that the dash-dotted lines connecting left and right parts of the diagram for scattering efficiency in Fig. 1(b) do not have anything to do with the dephasing of intermediate electronic states, but rather determine the type of the scattering process.

The character of electronic excitations plays the key role in the elastic scattering of light. Let us consider first the scattering via LEE's like, e.g., the states of excitons localized in the interface roughness potential. Because of the localized character of electronic state, there is no wave vector conservation in the vertices of interaction with incident and scattered light. Therefore, even in the lowest-order process of Fig. 1(a), the scattering may be, in principle, in any direction, because the information about the propagation direction of the incident photon cannot be transmitted into the scattered light through the LEE's. The only constraint on the wave vector of scattered light follows from the energy conservation and gives $|\vec{\kappa}_s| = |\vec{\kappa}_l|$. However, for a macroscopic collection of LEE's, the scattering pattern strongly depends on the spatial and/or energy distribution of the scattering centers. In fact, a regular lattice of identical LEE's necessarily leads to momentum conservation $\vec{\kappa}_s = \vec{\kappa}_l$, implying that a certain degree of disorder is required to obtain RRS from a collection of LEE's.

A totally different picture appears for the scattering by propagating states of excitons or uncorrelated electron-hole pairs in the process shown in Fig. 1(a). In this case, the matrix elements of interaction of the electronic subsystem with light (both incident and scattered) enforce the wave vector conservation. This leads immediately to the equation $\vec{\kappa}_s = \vec{\kappa}_l$ and, therefore, there is no elastic light scattering in directions different from that of the incoming photon (i.e., there is no RRS). The process of Fig. 1(a) for PEE's only contributes to the dressing of the photon Green function and is not the subject of our consideration. We, thus, conclude that the PEE's of a bulk semiconductor cannot produce the elastic scattering of light in the lowest-order perturbation theory. It is worth noting that the inclusion of the broadening of the PEE's does not change this picture: as shown in Fig. 1(c), the dressing of the electronic states is described by internal lines and does not contribute to the relaxation of the photon momentum conservation $\vec{\kappa}_l = \vec{\kappa}_s$.

In Fig. 1(b) we show processes where propagating intermediate electronic states are *elastically* scattered by, e.g., an impurity or interface roughness potential. We do not consider here the two-phonon vertices of interaction,[7] assuming that the temperature is low enough to neglect their contribution. However, a certain amount of impurities or other defects is a common feature of any real sample. The dash-dotted line in the diagram of Fig. 1(b) corresponds to the elastic interaction of PEE, with some kind of spatial disorder. The interaction with defects implies the relaxation of the strong constraint of the photon momentum conservation $\vec{\kappa}_l = \vec{\kappa}_s$ and the light can be scattered in all directions.

Thus, we have shown in this section that PEE's do not contribute to the elastic scattering of light in the lowest-order perturbation theory (see also Ref. 6). However, such scattering becomes possible via higher-order processes when some elastic mechanism is invoked to scatter intermediate electronic states in the sense of processes shown in Fig. 1(b). A single LEE leads to the isotropic Rayleigh scattering in the lowest order perturbation theory.

III. SCATTERING BY LOCALIZED ELECTRONIC STATES

In this section, we consider the RRS from a macroscopic ensemble of LEE's in the lowest-order perturbation theory [see Fig. 1(a)] and discuss different possible realizations of the energy and/or spatial LEE distribution. In particular, we analyze the case of distribution in a regular lattice with fluctuations in the position of localized states (we refer to as ordered array) and the two limiting cases of a completely random distribution (we refer to as disordered array) and of a perfect lattice. The inhomogeneous broadening is introduced by assuming a Gaussian distribution of the energies of individual localized states. Possible correlation effects in the energy fluctuations are not taken into account.

We consider the LEE's, which are homogeneously broadened by some mechanism of interaction like scattering by phonons [see Fig. 1(c)]. For the cases under consideration, we assume that all localized states contribute coherently to the total scattering amplitude. Hence, the contribution of each individual localized state has to be multiplied by the phase factor $\exp[i(\vec{\kappa}_l - \vec{\kappa}_s)\mathbf{r}_m]$ before squaring, where $\mathbf{r}_m$ is the position vector of localized state number m. One can see from the diagram on

Fig. 1(a), that the contribution $M(\Omega)$ from an individual localized state to the scattering amplitude is proportional to the propagator of electronic excitation:

$$M(\Omega_m) \sim G(\omega_l;\Omega_m) = (\omega_l - \Omega_m + i\Gamma_m/2)^{-1} , \quad (2)$$

where Ω_m (Γ_m) is the excitation energy (homogeneous broadening) of the state number m.

For an ideal three-dimensional (3D) lattice of *identical* LEE's states, the coherent sum of all contributions leads to the compensation of scattered waves in all directions besides that with $\vec{\kappa}_s = \vec{\kappa}_l$. This process contributes to the dressing of the photon propagator. There is no contribution to the Rayleigh scattering.

However, in the limit of disordered array the scattering efficiency is given by

$$I_s(\omega_l) \sim \delta(\omega_l - \omega_s)\Big[N|M(\Omega)|^2 + N(N-1)\delta_{\vec{\kappa}_l,\vec{\kappa}_s}|M(\Omega)|^2\Big] , \quad (3)$$

where N is the number of localized states. In Eq. (3), the first term describes the isotropic RRS, which comes out to be equal to the uncorrelated scattering from each localized state.

To be more general, let us introduce fluctuations in the *position* of identical LEE's arranged in a lattice (ordered array). For the lattice with Gaussian fluctuations, we found

$$I_s(\omega_l) \sim \delta(\omega_l - \omega_s)\Big\{N|M(\Omega)|^2 \times\Big[1 - \exp\Big(-\sum_{i=x,y,z}\frac{(\kappa_{li}-\kappa_{si})^2\Delta_i^2}{2}\Big)\Big] + N^2\delta_{\vec{\kappa}_l,\vec{\kappa}_s}|M(\Omega)|^2\Big\} , \quad (4)$$

where Δ_i is the spatial distribution width. The first term describes the Rayleigh scattering which is anisotropic because of the fluctuations. Equation (4) coincides with Eq. (3) and with the result for ideal lattice in the limit of $\Delta_i \to \infty$ and $\Delta_i \to 0$, respectively.

A very important difference in scattering from ordered and disordered arrays of LEE's appears when the energies of localized excitations are randomly distributed around some average value. This leads to inhomogeneous broadening of the resonance that has been observed in many optical investigations.[1,8,9,12] We assume a Gaussian form for these energy fluctuations. The RRS efficiency for the lattice of localized states with *energy and position* fluctuations is found to be

$$I_s(\omega_l) \sim \delta(\omega_l - \omega_s)\Big\{N\langle|M(\Omega)|^2\rangle_\Omega + N|\langle M(\Omega)\rangle_\Omega|^2\Big[N\delta_{\vec{\kappa}_s,\vec{\kappa}_l} - \exp\Big(-\sum_{i=x,y,z}\frac{(\kappa_{li}-\kappa_{si})^2\Delta_i^2}{2}\Big)\Big]\Big\} , \quad (5)$$

whereas for the totally disordered array of inhomogeneously broadened localized states,

$$I_s(\omega_l) \sim \delta(\omega_l - \omega_s)\left[N\langle|M(\Omega)|^2\rangle_\Omega + N(N-1)|\langle M(\Omega)\rangle_\Omega|^2\delta_{\vec{\kappa}_s,\vec{\kappa}_l}\right] . \quad (6)$$

In Eqs. (5) and (6) $\langle\rangle_\Omega$ represents the average over the Gaussian distribution of the energies of individual localized state around the energy Ω_0,

$$\langle f(\Omega)\rangle_\Omega = \frac{1}{\sqrt{\pi\Lambda^2}}\int_{-\infty}^{+\infty} d\Omega \exp\left(-\frac{(\Omega-\Omega_0)^2}{\Lambda^2}\right) f(\Omega), \quad (7)$$

where Λ is the distribution width.

Let us compare the contributions to the RRS ($\vec{\kappa}_s \neq \vec{\kappa}_l$, $\omega_s = \omega_l$) from the ideal lattice and a disordered array of inhomogeneously broadened LEE's. According to Eqs. (5) and (6), they are $N[\langle|M(\Omega)|^2\rangle - |\langle M(\Omega)\rangle|^2]$ and $N\langle|M(\Omega)|^2\rangle$, respectively. In both cases, the behavior of the scattering efficiency, as a function of the laser frequency ω_l, depends strongly on the relationship between homogeneous Γ and inhomogeneous Λ broadenings. The results of a calculation of the RRS efficiency evaluated with uncorrelated Gaussian distribution of local resonant frequencies are shown in Fig. 2. The calculations have been performed for a number of values of the parameter Γ^2/Λ^2 : $1 - 0.01; 2 - 0.04; 3 - 0.1; 4 - 0.2; 5 - 0.5; 6 - 2.0; 7 - 6.0; 8 - 20.0; 9 - 100.0$, assuming a constant Γ. We do not consider possible dispersion of Γ inside the inhomogeneous band. In the limit of a dominant inhomogeneous broadening, $\Lambda \gg \Gamma$, the cases of a perfect lattice and a disordered array give a very similar result. The spatial disorder does not play an important role and the RRS profile reflects the inhomogeneous energy distribution. However, dramatic differences are found in the opposite limit $\Lambda \ll \Gamma$. The RRS from totally disordered array [Fig. 2(a)] corresponds to the uncorrelated scattering from each localized state; it becomes independent of Λ and reflects the homogeneous profile [the dashed curve in Fig. 1(a) corresponds to the limit $\Lambda \to 0$]. The behavior is very much different for the lattice [Fig. 2(b)]: *the amplitude of the resonance acquires maximum at* $\Lambda \simeq \Gamma$ *and goes down for the further decreasing of* Λ. In the limit $\Lambda \to 0$, the scattering intensity is zero as it should be for an ideal lattice of identical LEE's.

In order to illustrate the resonant behavior by means of a simple equation and for the sake of comparison with other results,[1,2] we give the scattering efficiency of the lattice of localized states evaluated with a Lorentzian distribution of resonant energies:

$$I_s(\omega_l) \sim \delta(\omega_l - \omega_s)\left[\frac{(\omega_l-\Omega_0)^2-(\Theta^2-\Gamma^2)/4+(\Theta/\Gamma)[(\omega_l-\Omega_0)^2+(\Theta^2-\Gamma^2)/4]}{[(\omega_l-\Omega_0)^2+(\Theta^2+\Gamma^2)/4]^2-\Theta^2\Gamma^2/4}-\frac{1}{(\omega_l-\Omega_0)^2+(\Theta+\Gamma)^2/4}\right], \quad (8)$$

where Θ is the width of distribution centered at Ω_0. Under resonance conditions with the distribution center, $\omega_l = \Omega_0$, this simplifies to

$$I_s(\omega_l=\Omega_0) \sim \frac{4}{\Theta+\Gamma}\left(\frac{1}{\Gamma}-\frac{1}{\Theta+\Gamma}\right). \quad (9)$$

For $\Gamma \gg \Theta$, the intensity in the maximum is $(\Theta/\Gamma)(4/\Gamma^2)$ and the width of the resonant profile is equal to Γ. For $\Gamma \ll \Theta$, the maximum is $(\Theta/\Gamma)(4/\Theta^2)$ and the profile width is Θ. Note that the first term in the bracket of both Eq. (8) and Eq. (9) corresponds to the contribution from a disordered array. As stressed before, the difference between regular lattice and totally disordered array is negligible in the limit of $\Gamma \ll \Theta$. This means that, for large inhomogeneous broadening, the spatial distribution of LEE's is not important.

The dependence on the homogeneous and inhomogeneous broadenings in Eq. (9) is similar to that of Eqs. (3) and (4) of Ref. 1. However, its interpretation seems to be different. In Ref. 1, the contribution of two-dimensional excitons to the scattering efficiency has been evaluated via the dielectric response function. The authors refer to the paper of Loudon,[15] where the dielectric function for an isotropic dielectric medium (or for a cubic crystal) was calculated in the classical model for collection of damped, noninteracting, harmonic oscillators. Therefore, the theoretical analysis of Ref. 1 actually corresponds to the scattering from spatially homogeneous density of localized states with uncorrelated distribution of resonance energies. This explains why it is similar to our result for the lattice of localized states. However, the extension of this approach to the contribution from propagating electronic excitations, which is, in fact, assumed in Ref. 1, is not valid: as we have shown in the previous section, propagating states do not contribute to the Rayleigh scattering in the lowest-order perturbation theory.

We conclude this section by considering the layer semiconductor structure with localized electronic states being totally disordered along the layers that are arranged as a SL. Allowing for uncorrelated Gaussian fluctuations of the energy of localized states and the position of layers along the growth direction, we find

$$I_s(\omega_l) \sim \delta(\omega_l-\omega_s)\left(N_1N_2\left\{\langle|M(\Omega)|^2\rangle_\Omega - \delta_{\vec{\kappa}_{s\perp},\vec{\kappa}_{l\perp}}\exp[-(\kappa_{lz}-\kappa_{sz})^2\Delta_z^2/2]|\langle M(\Omega)\rangle_\Omega|^2\right\}+N_1^2N_2^2\delta_{\vec{\kappa}_s,\vec{\kappa}_l}|\langle M(\Omega)\rangle_\Omega|^2\right), \quad (10)$$

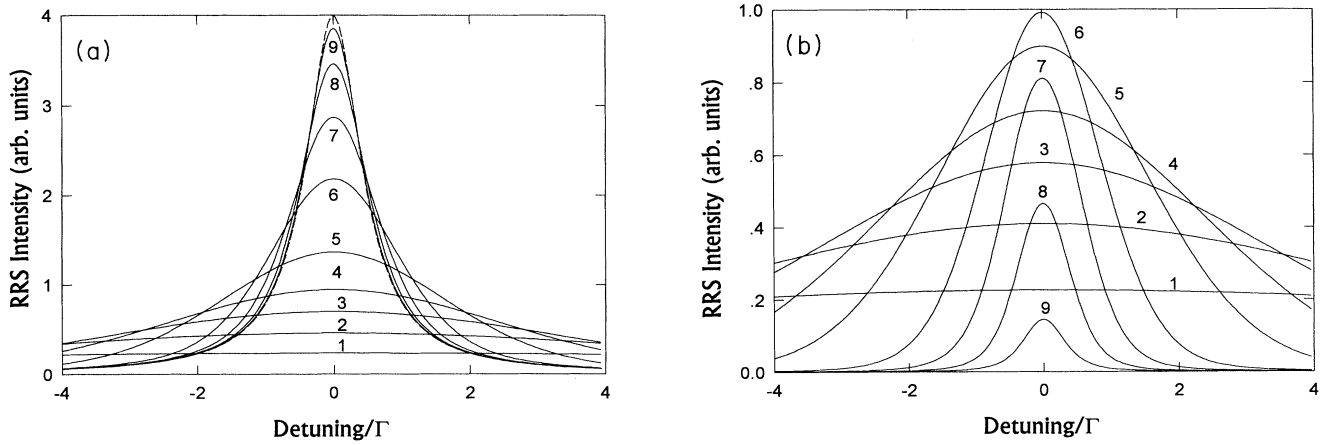

FIG. 2. The result of calculations of the scattering efficiency from (a) totally disordered and (b) ordered arrays of localized electronic states with Gaussian fluctuations in the energy of individual scattering centers. Detuning is taken with respect to the center of distribution. Different curves correspond to the different values of inhomogeneous broadening (see text for details).

where N_1 and N_2 are the number of localized states in the layer and the total number of layers, respectively. The first term in the square brackets contributes to the isotropic Rayleigh scattering. Taking into account the energy conservation, $c|\vec{\kappa}_s| = c|\vec{\kappa}_l|$, one sees that the term, proportional to the $\delta_{\vec{\kappa}_{s\perp},\vec{\kappa}_{l\perp}}$, gives a nonzero contribution only in the reflection and forward directions. The last term, proportional to the $\delta_{\vec{\kappa}_s,\vec{\kappa}_l}$, obviously represents the forward scattering. The model considered above may be related to multiple QW structures with a strong disorder when excitonic states are localized at random in the plane.

IV. SCATTERING BY PROPAGATING EXCITATIONS

We discuss in this section RRS by PEE's. As previously stated, this is only possible via higher-order processes, where intermediate states are elastically scattered by some kind of defects [see Fig. 1(b)]. From here on, we treat this scattering as uncorrelated interaction with impurities. In the case of interface roughness, relevant for QW structures, this corresponds to a roughness potential with infinitely small correlation length. An average over impurity positions recovers the translational invariance, and the corresponding components of the wave vector are conserved in the vertices of exciton- (electron, hole) impurity interaction. This means that the impurity line can carry out a well defined momentum. The intermediate electronic excitations are supposed to be the ground exciton states renormalized by all relevant interactions through the homogeneous broadening of propagators [Fig. 1(c)]. Models for single quantum well, bulk semiconductor, and multiple quantum-well structure are presented.

A. Single quantum well

In the lowest order perturbation theory [Fig. 1(a)], the quasi-two-dimensional character of propagating states ($\vec{\kappa}_{s\perp} = \vec{\kappa}_{l\perp}$) and the energy conservation ($|\vec{\kappa}_s| = |\vec{\kappa}_l|$) lead to the equation $\kappa_{sz} = \pm\kappa_{lz}$ for the wave vector components of the incident and scattered light perpendicular to the QW plane. Therefore, besides the forward scattering, there is a contribution to reflection. For an ideal infinite SL, the coherent sum over contributions of individual QW's compensates this term and there is only forward scattering (reflection from the sample surface is not discussed here).

In order to obtain the finite RRS efficiency for PEE's (in 1D, 2D, or 3D systems), one has to take into account the effect of disorder on the correlator of four current operators corresponding to the light scattering tensor. All possible diagrams with impurity (or random potential) external lines connecting electronic Green functions on the left and right hand sides of diagrams in Fig. 1(b) have to be added to those responsible for the dressing of a single-particle Green function considered in Ref. 13. We take account of all ladder contributions and assume that the disorder is weak enough to neglect all diagrams with crossing lines.

First, let us calculate the scattering efficiency from a single QW, taking the states of QW ground excitons as intermediate electronic excitations. We consider the disorder-induced scattering as interaction with 2D point defects with a potential $v_{e(h)}(\mathbf{r}) = v_{e(h)}(z)\delta(\mathbf{r}_\perp - \mathbf{r}_{\perp 0})$ for electrons and holes, respectively, where $\mathbf{r}_{\perp 0}$ describes the in-plane position of the impurity. The z dependence of the scattering potential is assumed to be the same for all impurities. The average over in-plane position of impurities recovers translational invariance. Therefore, the in-plane components of exciton wave vectors are conserved in all interaction vertices; for a single QW, the impurity lines in all diagrams of Fig. 1(b) do not carry the q_z variable. Evaluating the sum of all diagrams in Fig. 1(b), under the assumption $ka \ll 1$, where a is the exciton Bohr radius, we find

$$I_s(\omega_l) \sim \delta(\omega_l - \omega_s)|G_{\omega_0}(\kappa_{l\perp})|^2|G_{\omega_0}(\kappa_{s\perp})|^2 n_d\varepsilon^2 \times\left[1 - \frac{n_d\varepsilon^2 M}{\hbar^2} f(\omega_0,\omega_0)\right]^{-1}, \tag{11}$$

where

$$G_\omega(k) = \left[\hbar\omega_l - \hbar\omega - \frac{\hbar^2 k_\perp^2}{2M} + i\frac{\gamma_{\rm tot}}{2}\right]^{-1}, \tag{12}$$

$$f(\omega,\omega') = \frac{i + (2\pi)^{-1}\ln\{[\hbar\omega_l - \hbar\omega' - i\gamma_{\rm tot}(\omega_l - \omega')/2]/[\hbar\omega_l - \hbar\omega + i\gamma_{\rm tot}(\omega_l - \omega)/2]\}}{\hbar\omega' - \hbar\omega + i[\gamma_{\rm tot}(\omega_l - \omega) + \gamma_{tot}(\omega_l - \omega')]/2}. \tag{13}$$

M is the exciton mass, $\gamma_{\rm tot}$ is the total broadening of the exciton, n_d the areal concentration of defects, $\varepsilon = \varepsilon_e + \varepsilon_h$ is a sum of matrix elements for electron and hole evaluated with potential $v_{e(h)}(z)$ and size-quantized envelope wave functions, and $\hbar\omega_0$ is the excitonic gap.

The second term in square brackets in Eq. (11) can be written as

$$\frac{n_d\varepsilon^2 M}{\hbar^2} f(\omega_0,\omega_0) = \frac{\Gamma_d}{\gamma_{\rm tot}}\left[\frac{1}{2} + \frac{1}{\pi}\arctan\left(\frac{\omega_l - \omega_0}{\gamma_{\rm tot}/2}\right)\right] < 1, \tag{14}$$

where we have defined the quantity $\Gamma_d = n_d \varepsilon^2 M/\hbar^2$, related to the broadening γ_d of the excitonic state, due to scattering by defects by the relation

$$\gamma_d = \Gamma_d \Theta(\omega_l - \omega_0), \tag{15}$$

where $\Theta(\omega)$ is a Heavyside function.

The meaning of the term expressed by Eq. (14) should be qualitatively clear: it takes account of all contributions to the scattering efficiency with more than one external impurity line in Fig. 1(b). When the broadening $\gamma_{\rm tot}$ is mainly determined by processes other than the elastic scattering by defects, $\gamma_d/\gamma_{\rm tot} \ll 1$. This means that the probability of being elastically scattered in the sense of impurity line, connecting the left and the right sides of diagrams in Fig. 1(b), is very small compared to the inverse lifetime of the exciton. Obviously, the processes with multiple scattering of exciton by defects give then a negligible contribution to the RRS. However, in the case $\gamma_d \simeq \gamma_{\rm tot}$, the exciton lifetime is determined by the same interaction as that responsible for RRS and *all contributions in Fig. 1(b) are equally important.*

Note that for $\omega_l - \omega_0 \gg \gamma_{\rm tot}$, we have $f(\omega_0, \omega_0) \simeq 1/\gamma_{\rm tot}$ and

$$\Gamma_d f(\omega_0, \omega_0) \simeq \frac{\gamma_d(\omega_l - \omega_0)}{\gamma_{\rm tot}(\omega_l - \omega_0)} < 1 \,. \tag{16}$$

For $\omega_0 - \omega_l \gg \gamma_{\rm tot}$, one finds $f(\omega_0, \omega_0) \simeq 1/[2\pi(\hbar\omega_0 - \hbar\omega_l)]$ and

$$\Gamma_d f(\omega_0, \omega_0) \sim \Gamma_d/[2\pi(\hbar\omega_0 - \hbar\omega_l)] \ll 1 \tag{17}$$

is independent of $\gamma_{\rm tot}$. Thus, even without knowing the exact dependence of the $\gamma_{\rm tot}$ on frequency, we can tell that the function of Eq. (14) is asymmetric with respect to the excitation energy $\omega_l = \omega_0$. As we show below, this leads to the asymmetry and blueshift of the RRS profile.

Let us discuss the role of exciton dephasing in the RRS via PEE's. The dephasing enters the RRS efficiency via the $\gamma_{\rm tot}$ in Eqs. (12)–(14). In order to analyze the frequency dependence of the RRS intensity we approximate the total broadening $\gamma_{\rm tot} = \gamma' + \Gamma_d$ of the excitonic state by a constant, which can be separated into two terms: Γ_d, responsible for elastic scattering by defects and γ' which takes account of all inelastic scattering mechanisms. The RRS profiles, calculated from Eqs. (11)–(14) for different values of Γ_d/γ', while $\gamma' = 1$ in units of detuning, are reported in Fig. 3. In the limit $\gamma' \gg \Gamma_d$, the increase of disorder enhances the RRS efficiency without varying its near symmetric line shape. For $\Gamma_d \simeq \gamma'/3$ the elastic scattering of light reaches the maximum intensity and then, for a further increase of disorder, the RRS not only starts decreasing and broadening but even more relevant is the pronounced *asymmetry of its profile with a blueshift of the line from the central frequency* $\omega_l = \omega_0$. Therefore, RRS via PEE's turns out to be quenched in both limits of weak and strong disorder; in the last case, an asymmetry of the RRS profile with a blueshift is predicted.

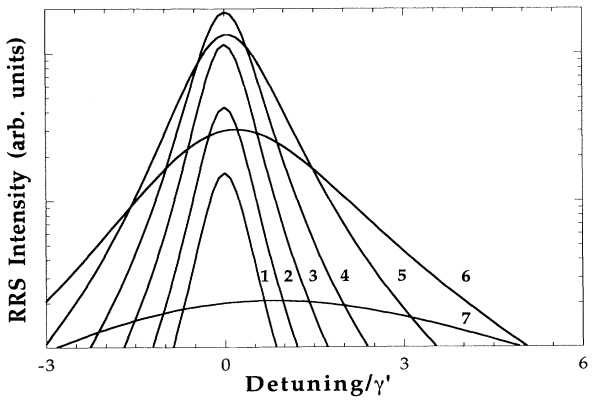

FIG. 3. The effects of disorder on the scattering efficiency via propagating excitonic states. Different curves correspond to the different values of Γ_d, while $\gamma' = 1$: (1) $\Gamma_d = 0.01$, (2) $\Gamma_d = 0.03$, (3) $\Gamma_d = 0.1$, (4) $\Gamma_d = 0.3$, (5) $\Gamma_d = 1$, (6) $\Gamma_d = 3$, (7) $\Gamma_d = 10$.

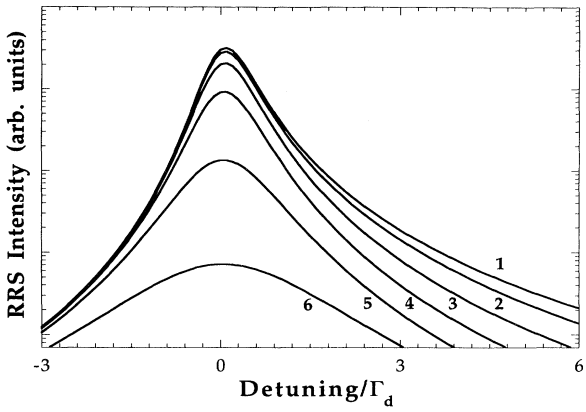

FIG. 4. The effects of dephasing on the scattering efficiency via propagating excitonic states. Different curves correspond to the different values of γ', while $\Gamma_d = 1$: (1) $\gamma' = 0.01$, (2) $\gamma' = 0.03$, (3) $\gamma' = 0.1$, (4) $\gamma' = 0.3$, (5) $\gamma' = 1$, (6) $\gamma' = 3$.

Other interesting information can be derived from the analysis of dependence of RRS on the broadening γ' of the excitonic states, due to all mechanisms except scattering by defects. In Fig. 4, we report the calculated RRS spectra for different values of the ratio γ'/Γ_d, while $\Gamma_d = 1$ in all cases. In the limit $\gamma' \ll \Gamma_d$, the RRS profile is asymmetric and blueshifted with respect to the excitonic transition $\hbar\omega_0$. Increasing γ', the RRS efficiency is quenched, the blueshift disappears and its line shape becomes broader and symmetric. Obviously, two of the most relevant mechanisms producing γ' are exciton-phonon and the exciton-exciton interaction; therefore, the trend shown in Fig. 4 may be related to the temperature and/or power dependence of RRS via PEE's.

B. Bulk semiconductor

The RRS efficiency by PEE's in bulk semiconductor can be obtained in a similar way. Formally, the result is the same as for a single QW, where one has to substitute

ε, ω_0, γ by corresponding bulk quantities:

$$I_s(\omega_l) \sim \delta(\omega_l-\omega_s)|G_{\omega_0}(\kappa_l)|^2|G_{\omega_0}(\kappa_s)|^2 n_d v^2 \times\left[1-\frac{n_d v^2}{2\pi\gamma_{\rm tot}}\left(\frac{2M}{\hbar^2}\right)^{3/2} \times{\rm Re}\sqrt{\hbar\omega_l-\hbar\omega_0+i\gamma_{\rm tot}/2}\right]^{-1}, \quad (18)$$

where n_d is now the bulk concentration of defects and $v = v_e + v_h$ is the strength of scattering potential $v_{e(h)}(\mathbf{r}) = v_{e(h)}\delta(\mathbf{r}-\mathbf{r}_0)$. The factor in the square brackets can be written as $1-(\gamma_d/\gamma_{\rm tot})$, similar to the case of a single QW.

C. Multiple quantum-well structure

We proceed to analyze the Rayleigh scattering from multiple QW structure, assuming the intermediate states as propagating in the plane of individual QW excitons. The ground exciton energy of individual QW's is allowed to fluctuate according to the Gaussian distribution. Such model corresponds to the large-scale disorder in the form of growth islands. The interface roughness, along with impurities, may also cause elastic scattering of the intermediate electronic states [see diagram in Fig. 1(b)]. We introduce, here, the scattering by point defects similar to the case of bulk semiconductor. After the proper average over impurity position, the in-plane component of wave vectors conserves in all vertices of interaction. A more sophisticated treatment should be taken over the wave vector component perpendicular to the growth direction. Although we deal in this section with a multiple QW structure, the electronic states are assumed to be localized in individual QW's. The conservation of the wave vector component along growth direction would appear as a result of the coherent sum of contributions to the RRS amplitude from all individual QW's. However, this happens only in a perfect multiple QW structure with a large enough number of periods. Since we consider here the structure with fluctuations in the well width, and corresponding fluctuations in the size-quantized energy of individual QW's, two types of contributions to the RRS efficiency appear: the one conserving the wave vector component along the growth direction and the other without such constraint. The second contribution is due to the inhomogeneous broadening.

According to Fig. 1(b), the nth order contribution to the RRS efficiency before averaging over the resonance energy distribution can be written as

$$I_s^{(n)}(\omega_l) \sim \sum_{q_{z1},\ldots,q_{zn}} \sum_{k_{\perp 1},\ldots,k_{\perp n-1}} \left|\sum_m M(\omega_{0m})\exp\left[i(\kappa_{lz}-\kappa_{sz}-Q_{zn})md\right]\right|^2 \delta(\omega_l-\omega_s), \quad (19)$$

where $Q_{zn} = \sum_{l=1}^{l=n} q_{zl}$, $M(\omega_{0m})$ is a contribution of mth QW to the total scattering amplitude, and d is the SL period. Averaging over the resonance energy and taking the sum over all individual QW's, we find

$$I_s^{(n)}(\omega_l) \sim \sum_{q_{z1},\ldots,q_{zn}} \sum_{k_{\perp 1},\ldots,k_{\perp n-1}} \left\{N\left[\left\langle|M(\omega)|^2\right\rangle_\omega - |\left\langle M(\omega)\right\rangle_\omega|^2\right] + N^2|\left\langle M(\omega)\right\rangle_\omega|^2\delta_{Q_{zn},\kappa_{lz}-\kappa_{sz}}\right\}\delta(\omega_l-\omega_s), \quad (20)$$

where $\langle\rangle_\omega$ was defined in Eq. (7) and N is the total number of QW's, assumed to be large enough for the condition $\sum_m \exp(ik_z md) \simeq N\delta_{k_z,0}$ to be satisfied.

Summing all diagrams in Fig. 1(b) we find

$$\begin{aligned} I_s(\omega_l) \sim v^2 n_d \frac{d}{b}\Bigg[&\left\langle|G_\omega(\kappa_{l\perp})|^2|G_\omega(\kappa_{s\perp})|^2\left[1-\frac{3Mv^2n_d}{2\hbar^3 b}f(\omega,\omega)\right]^{-1}\right\rangle_\omega \\ &-\left\langle\left\langle G_\omega(\kappa_{l\perp})G^*_{\omega'}(\kappa_{l\perp})G_\omega(\kappa_{s\perp})G^*_{\omega'}(\kappa_{s\perp})\left[1-\frac{3Mv^2n_d}{2\hbar^3 b}f(\omega,\omega')\right]^{-1}\right\rangle\right\rangle_{\omega,\omega'} \\ &+N\sum_{n=1}^{\infty}\sum_{q_{z1},\ldots,q_{zn}}\prod_{i=1}^{n}|\eta(q_{zi})|^2\delta_{Q_{zn},\kappa_{lz}-\kappa_{sz}} \\ &\times\left\langle\left\langle G_\omega(\kappa_{l\perp})G^*_{\omega'}(\kappa_{l\perp})G_\omega(\kappa_{s\perp})G^*_{\omega'}(\kappa_{s\perp})\left(\frac{3Mv^2n_d}{2\hbar^3 b}f(\omega,\omega')\right)^{n-1}\right\rangle\right\rangle_{\omega,\omega'}\Bigg], \end{aligned} \quad (21)$$

where b is the well width, $\langle\langle\rangle\rangle$ corresponds to the average over ω and ω' in the sense of Eq. (7) and $f(\omega,\omega')$ is given by Eq. (13).

The factor $\delta(\omega_l-\omega_s)$ has been omitted in Eq. (21). We used also the relation

$$\sum_{q_z}|\eta(q_z)|^2 = \frac{2b}{3Nd}\sum_{q_z}\left|\frac{\sin(q_z b/2)}{q_z b/2}\frac{4}{4-(q_z b/\pi)^2}\right|^2 = 1, \quad (22)$$

which is valid for a QW with infinitely high barriers.

All three contributions in Eq. (21) are of the same order in N, because of the δ symbol of Kronecker in the last term. The algebraic sum of the two first terms is not zero, only because of the inhomogeneous broadening. *The last (third) contribution is not zero even in the limit of negligible energy fluctuations.* The relationship between the first two and the last contribution of Eq. (21) is determined by the relationship between homogeneous and inhomogeneous broadenings.

Note that the first two terms of Eq. (21) result from the inhomogeneous broadening in the sense of spatial fluctuations in the size-quantized energy whereas the last one is an effect of disorder in the sense of Ref. 13 *on the light scattering tensor* (not on the propagator of electronic excitation) evaluated for scattering via PEE's.

V. EXPERIMENTAL EXAMPLES

We conclude by giving two experimental examples of RRS from a single QW and bulk semiconductor, respectively. Details of the experimental setup can be found elsewhere.[16] The single QW investigated is a MBE grown heterostructure consisting of a 90 Å GaAs layer sandwiched by thick $Al_{0.3}Ga_{0.7}As$ barriers. The RRS profile at T=8 K is reported in Fig. 5, together with the photoluminescence (PL) and photoluminescence excitation (PLE) spectra. The good optical quality of the sample is indicated by the 1.6 meV full width at half maximum (FWHM) of the PL spectrum. The most striking fact arising from the comparison of these spectra is the Stokes shift (SS) of the RRS, with respect to the PLE spectrum; a similar shift is also found for the PL band. We remark that the SS seems to be a general feature of the RRS in QW heterostructures: analogous results for RRS have been indeed reported in QW's of both higher[16] and lower[1] intrinsic quality. It is well known that the PL Stokes shift originates from the equilibrium distribution (trapping[17] or thermalization[18]) of the photogenerated excitons. Obviously, a different explanation must be invoked for RRS provided that the elastic scattering of light does not derive from the real exciton population. In fact, the physical origin of the SS in the RRS profile from a QW's has not yet been clarified and such a discussion is outside the aims of this paper. We refer to Ref. 16 for an analysis of the different possible explanations. Nevertheless, the presence of the SS implies that RRS from QW heterostructures essentially probe the excitonic states lying at the low energy side of the inhomogeneous absorption band and there is a general agreement on the localized character of these states.[1,19,16] Note also that our calculations for the RRS efficiency via propagating excitonic states eventually predict a blueshift of the RRS, with respect to the fundamental transition (in contrast to the SS observed in a QW).

The second example concerns the results of RRS from intrinsic bulk GaAs. The RRS profile at T=8 K is reported in Fig. 6 and compared with the PL and PLE spectra. The PL spectrum consists of three overlapping bands very well known in the literature; they correspond to the fundamental exciton (X, E=1.5153 eV), the exciton bound to neutral donor (D^0X, E=1.5141 eV), and the free hole–neutral donor transitions (D^0h, E=1.536 eV), respectively. Note the good quality of the sample, as inferred from the FWHM of 0.4 meV for the X line. Only the X transition is observed in the PLE spectrum, as expected since it essentially reflects the absorption, while both the X and D^0X contributions are found in the RRS profile. The presence of extrinsic transitions in the RRS spectrum, which are not usually detected in absorption, has been reported in QW structures[16] and in thin layers of ZnSeS,[19] as well, and is a clear indication to the fact that RRS tends to enhance the contribution from localized states. We see two possible reasons for the lack of D^0h in the RRS spectrum: (i) small population

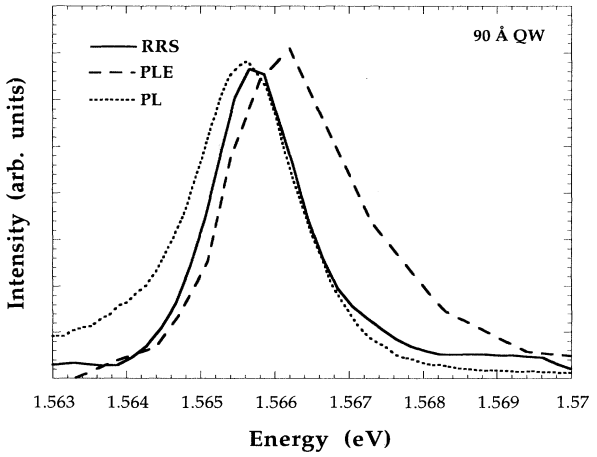

FIG. 5. Comparison of the RRS (solid line), PL (dotted line), and PLE (dashed line) spectra for a 90 Å QW at T=8 K.

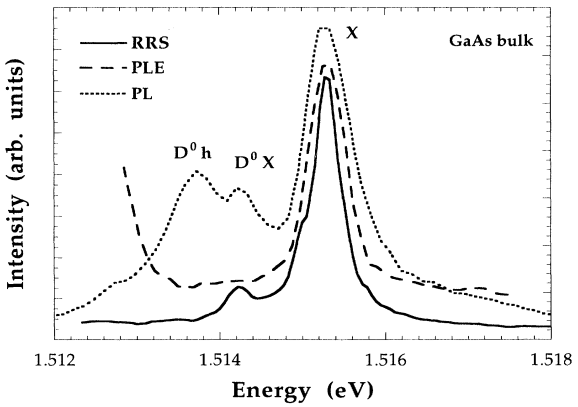

FIG. 6. Comparison of the RRS (solid line), PL (dotted line), and PLE (dashed line), spectra for bulk GaAs at T=8 K.

of the ionized donors at low temperature and (ii) nonresonant character of this process (the integral over the wave vector of a free hole state leads to a smooth behavior of the scattering efficiency in the vicinity of D^0h transition). However, at least to our purpose, the most interesting feature is the presence of the RRS from the fundamental exciton transition. In fact, this resonance is usually referred to as the *free exciton* in connection with its supposed propagating character. Our data, therefore, suggest that in bulk samples, the RRS may occur via PEE's. It should also be noted that from the undoped GaAs buffer layer on which the 90 Å QW investigated has been grown we find a RRS profile very similar to the one presented in Fig. 6, with an absolute intensity of the same order of magnitude as the RRS from the QW, even if the scattering volume in a bulk sample is roughly two orders of magnitude larger than in a QW. The much larger efficiency of the QW in producing RRS again suggests that the elastic light scattering occurs via different mechanisms in the two cases, that is, LEE in QW's and propagating exciton states in bulk semiconductors. Nevertheless, we would like to note that the disorder associated with impurity contamination can be effective to produce localization of the bulk exciton[20] and this is specially true for states with small wave vectors, such as the ones probed by RRS. We are unable to establish the propagating or localized character of the fundamental exciton in our bulk samples. However, we can definitely conclude that bulk samples are, when compared to the QW systems, better candidates for investigating the RRS via propagating excitonic states, very likely as a consequence of the absence of interface roughness, that is, the main origin of localization in QW's.

VI. CONCLUSIONS

To summarize, the relative role of propagating and localized electronic excitations, being intermediate states in the processes of resonant Rayleigh scattering, has been studied. It has been shown that only totally localized intermediate states lead to the elastic light scattering via the lowest-order processes. The effects of spatial and energy disorder have been analyzed. The scattering efficiency of an ordered and disordered arrays of localized states shows strongly different behavior as a function of inhomogeneous broadening. This dependence is monotonous for disordered array and it goes through a maximum for a lattice.

We have shown that the propagating electronic excitations only contribute to the elastic light scattering via higher-order processes. The scattering efficiency of the propagating excitons has been calculated for a single QW and for bulk semiconductor. The results show strong differences between the case when the exciton dephasing is determined by the same scattering mechanism as that responsible for light scattering, and the case when the broadening of excitonic states is due to some other stronger interaction. The scattering efficiency of a multiple quantum-well structure for scattering via propagating states of the exciton consists of two qualitatively different contributions. One of them results from the inhomogeneous broadening in the form of growth islands, whereas the other one is due to the elastic scattering of excitons by some defects or impurities in an otherwise perfect multiple quantum-well structure.

Finally, we have reported experimental results for a single QW and bulk GaAs. In the case of a QW, the presence of a SS of the RRS profile, with respect to the fundamental excitonic transition, denotes the prevailing of the elastic light scattering via localized states. It follows that in QW structures this experimental method is complementary to other coherent techniques, such as four wave mixing or hole burning. In the bulk case, instead, the RRS occurs exactly at the exciton transition, suggesting the possibility of a different scattering mechanism. Therefore, bulk materials seem to be better candidates, if compared to the more widely investigated QW systems, for studying RRS via propagating excitonic states. At the same time, RRS can be alternative to the above mentioned nonlinear techniques for studying dephasing processes in bulk semiconductor.

Note added in proof. Equation (8) can be simplified to

$$I_s(\omega_l) \sim \delta(\omega_l - \omega_s)\left(\frac{1}{\Gamma} - \frac{1}{\Theta+\Gamma}\right) \times \frac{\Theta+\Gamma}{(\omega_l - \Omega_0)^2 + (\Theta+\Gamma)^2/4}.$$

ACKNOWLEDGMENTS

The authors thank Professor M. Cardona for useful comments. V.I.B. and S.T.P. thank the European Union, and Ministerio de Educación y Ciencia de España (DGICYT) and the Russian Fundamental Investigation Fund (93-02-2362), respectively, for financial support and the University of Valencia for hospitality. This work has been partially supported by Grant No. PB92-1076 (DGICYT). Work at LENS was supported by the European Community under Contract No. GE1*/0046 Large Installation Plan.

* On leave from the P.N. Lebedev Physical Institute, Russian Academy of Science, Moscow, Russia.

[1] J. Hegarty, M. D. Sturge, C. Weisbuch, A. C. Gossard, and W. Wiegmann, Phys. Rev. Lett. **49**, 930 (1982).
[2] J. Hegarty, L. Goldner, and M. D. Sturge, Phys. Rev. B **30**, 7346 (1984).
[3] H. Stolz, D. Schwarze, W. von der Osten, and G. Weimann, Superlatt. Microstruct. **6**, 271 (1989).
[4] H. Stolz, D. Schwarze, W. von der Osten, and G. Weimann, Superlatt. Microstruct. **9**, 511 (1991).
[5] H. Stolz, D. Schwarze, W. von der Osten, and G. Weimann, Phys. Rev. B **47**, 9669 (1993).
[6] H. Stolz, in *Time-Resolved Light Scattering from Excitons*, edited by S. Flügge *et al.*, Springer Tracts in Modern Physics Vol. 130 (Springer-Verlag, Berlin, 1994), p. 72.
[7] M. Aihara, Phys. Rev. A **18**, 606 (1978).

[8] C. Weisbuch, R. Dingle, A. C. Gossard, and W. Wiegmann, Solid State Commun. **38**, 709 (1981).
[9] V. F. Sapega, V. I. Belitsky, T. Ruf, H. D. Fuchs, M. Cardona, and K. Ploog, Phys. Rev. B **46**, 16 005 (1992).
[10] T. Ruf, V. I. Belitsky, J. Spitzer, V. F. Sapega, M. Cardona, and K. Ploog, Phys. Rev. Lett. **71**, 3035 (1993).
[11] D. N. Mirlin, I. A. Merkulov, V. I. Perel, I. I. Reshina, A. A. Sirenko, and R. Planel, Solid State Commun. **84**, 1093 (1992).
[12] T. Ruf, J. Spitzer, V. F. Sapega, V. I. Belitsky, M. Cardona, and K. Ploog, Phys. Rev. B **50**, 1792 (1994).
[13] S. Glutsch and F. Bechstedt, Phys. Rev. B **50**, 7733 (1994).
[14] S. T. Pavlov, Dr. Sci. Thesis, St. Petersburg University, 1978; E. L. Ivchenko, I. G. Lang, and S. T. Pavlov, Fiz. Tverd. Tela (Leningrad) **19**, 1751 (1977) [Sov. Phys. Solid State **19**, 718 (1977)].
[15] R. Loudon, J. Phys. A **3**, 233 (1970).
[16] M. Gurioli, F. Bogani, A. Vinattieri, M. Colocci, V. I. Belitsky, A. Cantarero, and S. T. Pavlov, Solid State Commun. (to be published).
[17] F. Yang, M. Wilkinson, E. J. Austin, and K. P. O'Donnel, Phys. Rev. Lett. **70**, 323 (1993).
[18] M. Gurioli, J. Martinez Pastor, A. Vinattieri, and M. Colocci, Solid State Commun. **91**, 931 (1994); Phys. Rev. B **50**, 11 817 (1994).
[19] H. Stolz, in *Time-Resolved Light Scattering from Excitons* (Ref. 6), p. 174.
[20] V. M. Agranovich, V. E. Kravtsov, and I. V. Lerner, Phys. Lett. A **125**, 435 (1987).